2020 17th International Conference on Ubiquitous Robots (UR)
June 22-26, 2020. Kyoto, Japan

Minimal Degree of Freedom Dual-Arm Manipulation Platform with Coupling Body Joint for Diverse Cooking Tasks

Donghun Noh[1], Yeting Liu[1], Fadi Rafeedi[1], Hyunwoo Nam[1], Kyle Gillespie[1], June-sup Yi[2], Taoyuanmin Zhu[1], Qing Xu[1], and Dennis Hong[1]

Abstract— **This paper introduces the kinematic configuration, kinematic analysis, workspace analysis of a dual-arm manipulation platform intended for varied cooking applications. Based on the analysis of different essential cooking tasks, each arm was designed to have 5 degrees of freedom (DOFs) independently with an additional single DOF located at the center of the linkage connecting the two arms. The additional actuator expands the reachable workspace as well as the common workspace between the two arms. Furthermore, the additional joint optimizes the arm's joint configuration for cooking tasks by giving the arm a redundant pitch joint. This allows the ends of each arm to be able to produce linear planar trajectories which are important for many precise cooking actions. The system will also be able to multitask, being able to simultaneously perform potentially disparate tasks in different areas of its workspace. Besides these advantages, we expect that this dual-arm system will be more computationally and cost-efficient than similar systems using higher DOF arms.**

I. INTRODUCTION

As technology in robotics advances, robots have begun to be increasingly utilized in everyday life. Among the different types of robots, robotic manipulators especially have been developed in order to perform our most labor-intensive tasks. As such, a wide variety of manipulators have been developed ranging from low degree of freedom (DOF) manipulators for simple tasks such as pick and place operations, to high degree of freedom manipulators for complex tasks in which joint redundancy is needed such as in the stirring and plating of food [1],[2]. Cooking is a prime example of an exciting area for the application of automation. As our lives become ever more rushed, it is becoming increasingly more difficult to spare the time to cook high quality, healthy, and delicious meals for ourselves. However, in spite of numerous attempts to develop a manipulator capable of quickly, reliably, and affordably producing a variety of restaurant quality meals, the results have primarily been limited to single-taskers, which are only able to produce a single type of dish, and basic human cooperative robots, which are unable to multitask due to technical challenges in developing a cooking system compatible with said cooperation [3], [4], [5], [6], [7]. To overcome these challenges, developing a cooking robot with a high DOF in a well-organized kitchen has been tried by Octochef [8], Moley [9], Samsung Bot Chef [10], LG CLOi Chefbot [11], and Misorobotics Flipy [12]. As the basic processes required for cooking are dynamically complicated tasks that a human arm is doing, these cooking robots have arms with more than 6 degrees of freedom (DOFs) which is similar to the DOFs of a human arm. Although the high degree of freedom manipulators have been used, they still face a lot of problems, such as their computational complexity, geometric complexity, and environmental uncertainty, which need to be solved for a practical cooking robot to properly operate in reality.

TABLE I. Essential Cooking Tasks and DOFs

	Task Type	DOFs
1	Simple Cutting	2
2	Stir Frying	4
3	Mixing	3
4	Pan Manipulation	2

This paper presents the kinematic configuration of a new design of a dual arm manipulation platform which has the optimized structure especially for cooking tasks to simplify the control problems. The design consists of two 5 DOF arms coupled together and allowed to rotate about its body's central axis by an additional 11th joint at its center. A diagram representing this layout is given in Fig. 1. We assume that this newly designed manipulator will operate in a structured environment. Said structured environment is a pre-planned kitchen in which the tools and kitchen appliances the robot will interact with are housed in specific and consistent locations. Furthermore, the cooking table, tools, and appliances are optimally arranged in consideration with the manipulator's orientation.

When first approaching this design challenge we first considered what was the least complex solution that would still effectively completing the requirements. On this premise, we began to research which cooking tasks our system would need to be able to complete to function fully. Table I shows the required DOFs for essential cooking tasks [13], [14], [15] as well as the fact that most of cooking tasks can be done using 4 or fewer DOFs. This lead to the choice of designing a 5DOF arm in order to meet these requirements while still providing a reasonable workspace.

Using 5 DOF arms offers many favorable advantages. They have lower expected computational complexities required for their control as well as increased end-effector positional accuracy due to their simpler structure [16], [17].

*This research was supported by Woowa Brothers Corporation.

[1]All authors are with the Robotics and Mechanisms Laboratory (RoMeLa) at the University of California, Los Angeles (UCLA), Los Angeles, CA 90095, USA. The corresponding author can be reached at donghun.noh@ucla.edu

[2]June-sup Yi, Sungkyunkwan University, 2066 seobu-ro, Suwon-si, Jangan-gu, Gyeonggi-do, Republic of Korea

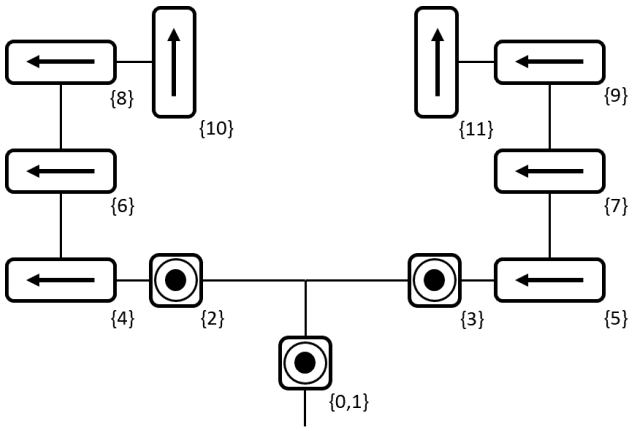

Fig. 1. Top View of the Joint Configuration of the Dual-Arm Manipulator

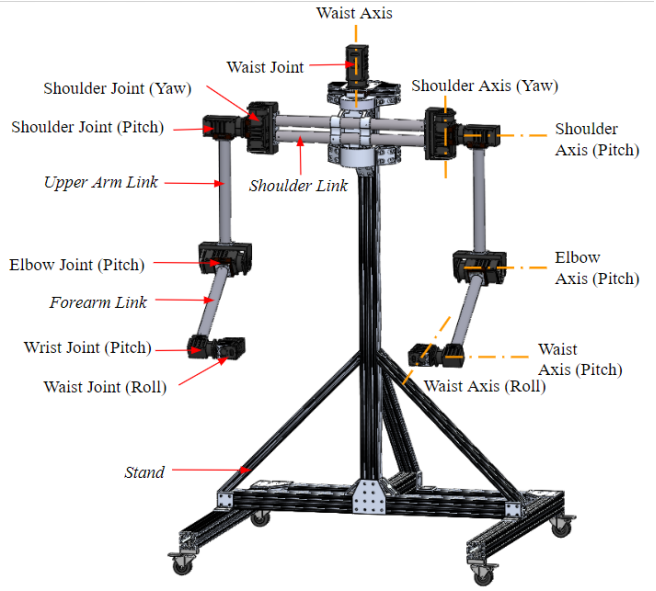

Fig. 2. 3D CAD Model of the Dual-Arm Manipulator

Although 5 DOFs arms have controllable, structural, cost efficient advantages, their lack of redundancy can be fatal. It must be noted though that having only 5 DOFs limits the robot's ability to orient its manipulators which could be considered to be a significant disadvantage in some cooking operations. This is addressed in two ways. Firstly, an additional shared sixth degree of freedom was added to the base of the robot allowing the two connected arms to rotate about the platform's base. This allows for the robot to add some additional reachable orientations to each end-effector and allows for some unique possible end-effector trajectories such as moving linearly within a plane. In addition, this shared sixth degree let the robot utilize multiple sides of the kitchen at the same time. Furthermore, by adding this extra degree of freedom, the arm could have redundancy in pitch direction which is necessary for diverse tasks to avoid objects caused by the structure properties of kitchen such as layered shelves and deep storage space. Secondly, as mentioned above, through creating a structured kitchen environment for the robot to work in. This allows us to minimize the concerns of limited control over end-effector orientation by assuring that each task will be performed in the optimal location for the required manipulator orientation.

The following sections will discuss the design and analysis of this new robotic system. Section 2 will discuss the considerations taken in the mechanical design of the arms and body of the robot. Section 3 will analyze the kinematic equations and Section 4 will examine workspace of the system. And section 5 will demonstrate through simulation some of the different applications of the system.

II. Mechanical Design Considerations

A. Manipulator Platform Design

The dual-arm manipulation platform has two arms connected by a shoulder link and a stand with caster wheels on the bottom. Each of the cooking robot's five DOF arm has the first two DOFs (Yaw followed by pitch) located on the shoulder and orthogonal to each other. The third DOF (Pitch) is located on the elbow and then two additional DOF's (Pitch followed by Roll) are located on the wrist. Actuators at each joint are interconnected in series by arm linkages. Having a five DOF arm design reduce the weight and inertia of the arm, and make the cooking robot more energy efficient and cost-effective, and is expected to be easier to control with simpler trajectory planning. Additionally, there is another rotational joint at the junction of the robot's torso and shoulder so that the entire shoulder can rotate.

In order to design a human-sized cooking robot, the lengths of upper arm and forearm links of the dual-arm manipulation platform are set to 304.8 mm (one foot), and the shoulder link length is 450 mm. The total height of the manipulation platform is about 1450mm. This ensures the dual-arm manipulation platform has a decent reachable workspace, and the overlap of the arms' workspaces is large enough to perform dual-arm manipulation tasks comfortably. Moreover, with the help of the extra DOF in the platform's waist, the reachable workspace of the dual-arm manipulation platform covers most of the planned structured cooking environment. Carbon fiber was chosen as the material to make up the arm and shoulder linkages due to its ability to provide a high stiffness and a light weight to the arm. The full, annotated CAD model of the design made in SolidWorks is shown above in Fig. 2.

B. Payload and Torque Requirements

The minimum torque requirement for each actuator is obtained through a static moment balance approach. As a body becomes balanced about a pivot point, the resulting torque from each side of the pivot must be equal. When the arm reaches the pose with a fully extended arm in horizontal direction, the required torque from each actuator will be at their maximum values. This worst case scenario will be used as a reference for choosing the appropriate actuators. For the estimation of torque requirements, a general payload requirement for cooking was taken into consideration. It is

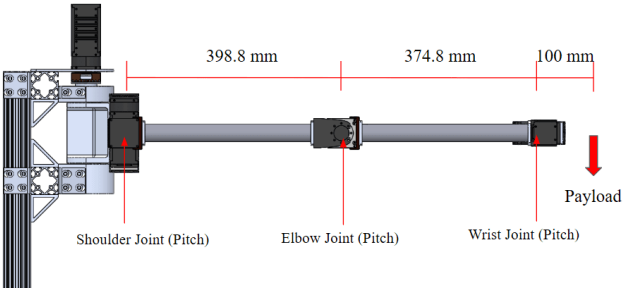

Fig. 3. Pose with Fully Extended Arm in Horizontal Direction

assumed that there is a 2kg payload attaching to the end-effector which is 100 mm away from the wrist joint, and the lengths between the shoulder, elbow and wrist joint are 398.8 mm and 374.8 mm respectively (as shown in Fig. 3). Moreover, the actuators at the shoulder and elbow joints are assumed to weigh 1 kg each and the actuators at the wrist joint are considered to have the weight of 0.5 kg. After the minimum torque requirements are obtained from the static moment balance approach, a safety factor of 1.5 needs to be considered to compensate the extra torque from inertial effects, which carries out the general torque requirements for each pitch actuator (as shown in Table II).

TABLE II. Torque Requirement for Each Pitch Actuator

Actuator	Shoulder Joint (Pitch)	Elbow Joint (Pitch)	Wrist Joint (Pitch)
Torque Requirement (N·m)	37.21	17.65	2.94

C. Prototype Manufacturing

A prototype was developed to test the configuration and workspace of the design in a real environment. Based on the torque requirement analysis in the previous section, Dynamixel Pro Plus actuators from Robotis are used. Dynamixel PH42-020-S300-R has a continuous torque of 5.1 N·m and weighs 340 grams, which is enough for the pitch actuator in the wrist joint. Dynamixel PH54-200-S500-R has a much greater continuous torque of 44.7 N·m with a weight of 855 grams and is suitable for the pitch actuators in the shoulder and elbow joints. Furthermore, for easier installation and control, the Dynamixel PH54-200-S500-R was also chosen as waist actuator and yaw actuator at shoulder joint, and Dynamixel PH42-020-S300-R is used as the roll actuator at wrist joint. With the chosen actuators above, the weight of the single arm is 4.39 kg, and the dual arm manipulator weighs 11.12kg when including the shoulder link in the middle.

From the described design, the dual-arm manipulation platform prototype was fabricated, shown in Fig. 4. All parts were manufactured in-house.

III. KINEMATICS ANALYSIS

A. Forward Kinematics

The forward kinematics of a robot calculates the position and orientation of its end-effector frame relative to its base frame based on its joint angles. Here, the Denavit-Hartenberg (D-H) representation is used to represent the forward kinematics. The forward kinematics of the left arm is presented in this section, and as the right arm has a mirrored configuration, the forward kinematics of the right arm can be done similarly.

Fig. 4. Dual-Arm Manipulation Platform

The assigned orientations of all joint frames is shown below in Fig. 5. It should be noted that, the base frame is defined at the robot's torso and that the last two joints are combined at the intersection point of those two joint axes. The linkage frames are established based on D-H rules, and the corresponding D-H parameters are shown in Table IV.

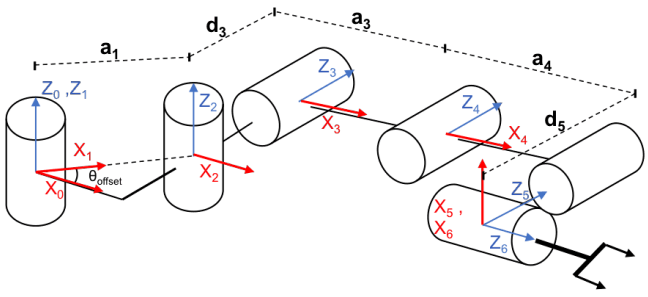

Fig. 5. Left Arm Frame Assignment for DH Parameters

TABLE III. Constant Parameters for Frames

Symbol	Values
a_1	0.2886m
a_3	0.3988m
a_4	0.3748m
d_3	0.1020m
d_5	-0.0840m
θ_{offset}	75.96°

TABLE IV. D-H Parameters of the Left Arm

Link	a_{i-1}	α_{i-1}	d_i	θ_i
1	0	0	0	$\tilde{\theta}_1$
2	a_1	0	0	$\tilde{\theta}_2$
3	0	$-\pi/2$	d_3	θ_3
4	a_3	0	0	θ_4
5	a_4	0	d_5	$\theta_5-\pi/2$
6	0	$-\pi/2$	0	$-\pi/2$

Note that $\tilde{\theta}_1 = \theta_1 + \theta_{offset}$ and $\tilde{\theta}_2 = \theta_2 - \theta_{offset}$. Also consider that d_5 in Table III is -0.0840m because it is the distance from $\mathbf{X_4}$ to $\mathbf{X_5}$ measured along $\mathbf{Z_5}$.

The homogeneous transformation matrix between adjacent link frames is defined as:

$$ {}^{i-1}_{i}T = \begin{bmatrix} c_i & -s_i & 0 & a_{i-1} \\ s_i c\alpha_{i-1} & c_i c\alpha_{i-1} & -s\alpha_{i-1} & -s\alpha_{i-1} d_i \\ s_i s\alpha_{i-1} & c_i s\alpha_{i-1} & c\alpha_{i-1} & c\alpha_{i-1} d_i \\ 0 & 0 & 0 & 1 \end{bmatrix} $$

where c_i and s_i represent $\cos\theta_i$ and $\sin\theta_i$, respectively.

The Cartesian position and orientation of the end-effector relative to the base frame is computed by ${}^{0}_{6}T$, which is a function of all joint variables. ${}^{0}_{6}T$ is computed and presented below:

$$ {}^{0}_{6}T = {}^{0}_{1}T\,{}^{1}_{2}T\,{}^{2}_{3}T\,{}^{3}_{4}T\,{}^{4}_{5}T\,{}^{5}_{6}T $$

$$ {}^{0}_{6}T = \begin{bmatrix} r_{11} & r_{12} & r_{13} & P_x \\ r_{21} & r_{22} & r_{23} & P_y \\ r_{31} & r_{32} & r_{33} & P_z \\ 0 & 0 & 0 & 1 \end{bmatrix} $$

where $r_{11} = s_{12}s_6 + c_{12}s_{345}c_6$, $r_{12} = s_{12}c_6 - c_{12}s_{345}s_6$, $r_{13} = c_{12}c_{345}$, $r_{21} = s_{12}s_{345}c_6 - c_{12}s_6$, $r_{22} = -s_{12}s_{345}s_6 - c_{12}c_6$, $r_{23} = s_{12}c_{345}$, $r_{31} = c_{345}c_6$, $r_{32} = -c_{345}s_6$, $r_{33} = -s_{345}$, $P_x = a_1c_1 + a_3c_{12}c_3 + a_4c_{12}c_{34} - d_3s_{12} - d_5s_{12}$, $P_y = a_1s_1 + a_3s_{12}c_3 + a_4s_{12}c_{34} + d_3c_{12} + d_5c_{12}$, $P_z = -a_3s_3 - a_4s_{34}$.

B. Inverse Kinematics

Inverse kinematics is used to control the movement of a robotic arm through the calculation of the required joint angles needed for the end-effector frame to reach a chosen position and orientation with respect to its base frame. In this section the inverse kinematics are obtained analytically. This solution gives all the possible solutions of the inverse kinematics. This enables us to choose the optimal path of the manipulator based on its initial state and the surrounding environment.

To solve the inverse kinematics, we will consider a given orientation and position of the end-effector ${}^{B}_{E}P$ and ${}^{B}_{E}R$ respectively. The goal position can be represented as:

$$ {}^{B}_{E}T = \begin{bmatrix} r_{11} & r_{12} & r_{13} & P_x \\ r_{21} & r_{22} & r_{23} & P_y \\ r_{31} & r_{32} & r_{33} & P_z \\ 0 & 0 & 0 & 1 \end{bmatrix} = \begin{bmatrix} {}^{B}_{E}R & {}^{B}_{E}P \\ 0 & 1 \end{bmatrix} $$

To get the inverse kinematics, the following equation will be solved,

$$ {}^{B}_{E}T = {}^{0}_{6}T \tag{1} $$

First, the dependence on $\tilde{\theta}_1$ will be placed on the left hand side of equation (1) as follows,

$$ \left[{}^{0}_{1}T\right]^{-1} {}^{B}_{E}T = {}^{1}_{6}T \tag{2} $$

Next, following equations can be obtained by using (2).

$$ r_{31} = c_6c_{345}, r_{32} = -s_6c_{345}, r_{33} = -s_{345} $$

Thus, θ_6 and the combined angle $\theta_{345} = \theta_3 + \theta_4 + \theta_5$ can be decided as (3) and (4).

$$ \theta_3 + \theta_4 + \theta_5 = Atan2\left(-r_{33}, \mp\sqrt{r_{31}^2 + r_{32}^2}\right) \tag{3} $$

$$ \theta_6 = Atan2\left(-r_{32}/\cos\theta_{345}, r_{31}/\cos\theta_{345}\right) \tag{4} $$

Similarly, by placing the dependence on both $\tilde{\theta}_1$ and $\tilde{\theta}_2$ on the left hand side of (1), we can solve for both $\tilde{\theta}_1$ and $\tilde{\theta}_2$

$$ \left[{}^{1}_{2}T\right]^{-1} \left[{}^{0}_{1}T\right]^{-1} {}^{B}_{E}T = {}^{2}_{6}T \tag{5} $$

Using (5) the following can be obtained

$$ \tilde{s}_{12} = \frac{c_6s_{345}r_{22} + s_6s_{345}r_{21}}{r_{11}r_{22} - r_{21}r_{21}} = a $$

$$ \tilde{c}_{12} = \frac{-c_6c_{345}r_{12} + s_6s_{345}r_{22}}{r_{11}r_{22} - r_{12}r_{22}} = b $$

$$ \tilde{\theta}_1 + \tilde{\theta}_2 = \theta_1 + \theta_2 = Atan2(a, b) \tag{6} $$

Since the expression $\theta_1 + \theta_2$ is now known, it can be used to obtain θ_2 using,

$$ \tilde{s}_2 = \frac{d_5 + d_3 + P_xs_{12} - P_yc_{12}}{a_1} = c $$

Thus,

$$ \tilde{\theta}_2 = Atan2\left(c, \pm\sqrt{1 - c^2}\right) $$

$$ \theta_2 = Atan2\left(c, \pm\sqrt{1 - c^2}\right) + \theta_{offset} \tag{7} $$

and,

$$ \theta_1 = Atan2(a, b) - Atan2\left(c, \pm\sqrt{1 - c^2}\right) - \theta_{offset} \tag{8} $$

Again using (5) we can write the following equations

$$ P_xc_{12} + P_ys_{12} - a_1\tilde{c}_2 = a_4c_{34} + a_3c_3 $$

$$ -P_xs_{12} + P_yc_{12} + a_1\tilde{s}_2 = a_4c_{34} + a_3c_3 $$

$$P_z s_{12} = -a_4 s_{34} - a_3 s_3$$

By squaring the previous three equations and summing them we can write isolate $cos(\theta_4)$ and write θ_4

$$\theta_4 = Atan2\left(\pm\sqrt{1-c_4^2}, c_4\right) \tag{9}$$

Finally, we place the dependence on $\tilde{\theta}_1$, $\tilde{\theta}_2$ and θ_3 on the left side of (1)

$$\left[{}^2_3T\right]^{-1}\left[{}^1_2T\right]^{-1}\left[{}^0_1T\right]^{-1}{}^B_E T = {}^3_6T \tag{10}$$

Using (10), we can come up with the following expressions.

$$d\cos\theta_3 + e\sin\theta_3 = f$$
$$g\cos\theta_3 + h\sin\theta_3 = i$$

Where,

$$d = P_x c_{12} + P_y s_{12} - a_1\tilde{c}_2$$
$$e = -P_z$$
$$f = a_3 + a_4 c_4$$
$$g = -P_z$$
$$h = -P_x s_{12} + P_y c_{12} + a_1\tilde{s}_2$$
$$i = a_4 s_4$$

And then, solve for θ_3

$$\theta_3 = Atan2\left(di - df, fh - ei\right) \tag{11}$$

Lastly, we can calculate θ_5 using (3), (9), and (11).

$$\theta_5 = Atan2\left(-r_{33}, \pm\sqrt{r_{31}^2 + r_{32}^2}\right) - \theta_4 - \theta_3 \tag{12}$$

IV. WORKSPACE ANALYSIS

TABLE V. Angle Range of Each Actuator

Actuator	Minimum Angle (°)	Maximum Angle (°)
Shoulder Yaw	-110	110
Shoulder Pitch	-180	180
Elbow Pitch	-125	125
Wrist Pitch	-180	180
Wrist Roll	-90	90
Waist	-100	100

In order to plan the actuators' motions in each cooking process and generate the proper trajectories, knowing the reachable workspace of this dual-arm manipulation platform is the first priority. Regardless of the end-effector and its shape, the reachable workspace for the 5 DOF single arm is determined by the first three joints, which are the shoulder yaw, shoulder pitch, and elbow pitch joints. To find the total reachable workspace of the full dual-arm manipulation platform, the waist joint must also be considered. Before approaching the workspace of the cooking robot, it is necessary to obtain the range of motion for each joint in the manipulator (Table V), which will define the inner and outer boundaries of the reachable workspace.

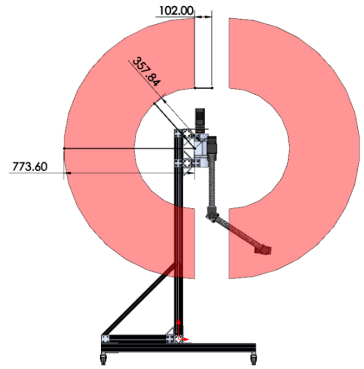

Fig. 6. Reachable Workspace in the Horizontal Plane

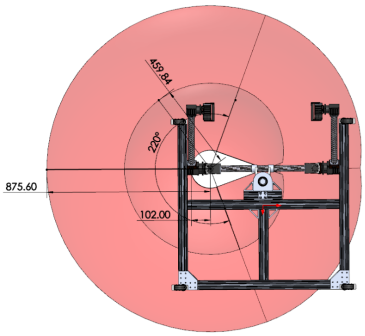

Fig. 7. Reachable Workspace in the Vertical Plane

As the shoulder yaw and shoulder pitch remain fixed, the rotation of the elbow joint would produce an arc segment. Then, as the shoulder pitch rotates freely, numerous arc segments can be created, which when combined will produce a hollow circle in 2D space. Furthermore, the range of movement of the shoulder yaw joint will make this hollowed circle into a hollow sphere in 3D space, which is the total reachable workspace of the single 5 DOF arm. For easier visualization, side views from its horizontal and vertical planes are presented below in Fig. 6 and Fig. 7, as well

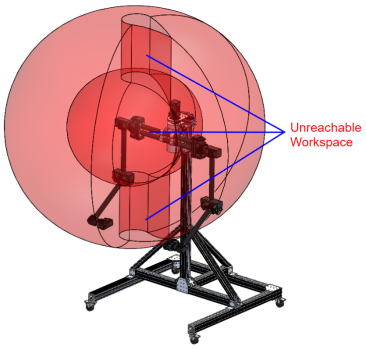

Fig. 8. Isometric View of the Reachable Workspace

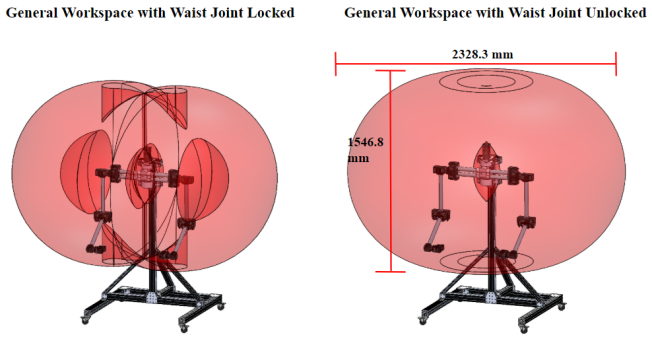

Fig. 9. Reachable Workspace of the Cooking Robot with and without the Waist Joint Locked

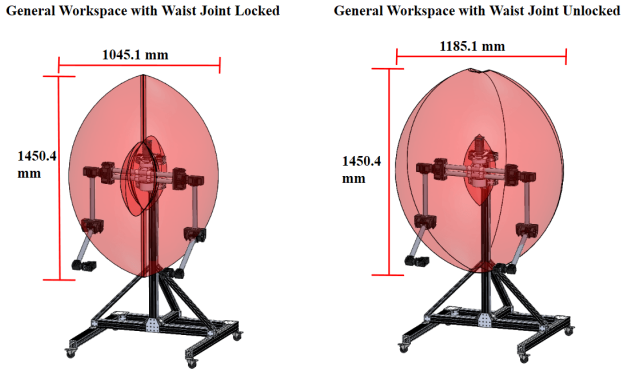

Fig. 10. Common Workspace of the Cooking Robot

as the isometric view in Fig. 8.

As for the full reachable workspace of the dual-arm manipulation platform, first we can apply the same method to get the reachable workspace of the second arm, this is shown in Fig. 9. Next, with the help of the central body joint, the reachable workspace of the cooking robot is swept around its axis as is shown in Fig. 9, and the manipulator is able to reach most of its surrounding area. The addition of the body joint allows for a larger and more uniform workspace, greatly simplifying considerations of processes which may be taking place on the outer edge of the system's workspace.

When the robot is performing cooking processes, it is normal for the system to use both arms for a single task, such as chopping or dicing an ingredient while holding it in place or stirring a soup while stabilizing the bowl it is in. Therefore, it is necessary for the robot to have significant overlap in the reachable workspaces of each of the cooking robots arms. This shared workspace is often referred to as the common workspace. With a greater common workspace comes a larger area for the cooking robot to perform dual-arm tasks. In order for the cooking robot to be fully functional in all areas of the kitchen, it is vitally important that the common workspace exists in all sections of the cooking environment. Typically, this is not possible in even 6 DOF arm systems due to limitations in the reach of the arms. Even when optimized, the common workspace is constrained to directly in front and back of the arms and is relatively small [18]. This limited version of the common workspace for our manipulator when the body joint is locked is shown on the left in Fig. 10. With this configuration, the manipulator's arms would only be able to operate cooperatively directly in front of it. However, with the central body joint providing rotation to the arms, the common workspace can be rotated about the robot's axis. This allows for the effective common workspace, seen in Fig. 10, to be swept around the body of the robot into a rounded diamond shape providing full functionality on all working surfaces.

V. Task Simulations

To demonstrate the capabilities the robot was designed for, we aimed to simulate 3 tasks: making parallel cuts with a knife, stir-frying with a pan, and demonstrating multitasking in different perpendicular work areas. These illustrate the ability of the robot to follow precise linear trajectories in plane, follow more complex planar circular and human like trajectories, and to easily and efficiently operate in a complex working environment respectively. Being able to accomplish all of these tasks distinguishes this system from simple single tasking cooking robots and can be completed with greater ease and efficiency than other similar dual arm systems which employ 6 DOF arms and lack a central body joint.

One of the most prevalent tasks in cooking is the cutting, slicing, and dicing of ingredients. While it is common, it is far from straightforward. It requires close precision and accurate force management and is a skill humans need to be carefully trained in. Applying robotics to cutting and dicing ingredients in semi-structured cooking environments continues to be a challenge addressed by the scientific community. Recent advancements have come in the form of improving the technique and force feedback [13], modeling of easily deformable ingredients [19], and in applying computer vision to aid in the feedback process [20]. Future work will focus on applying these concepts to our own system. For this paper,

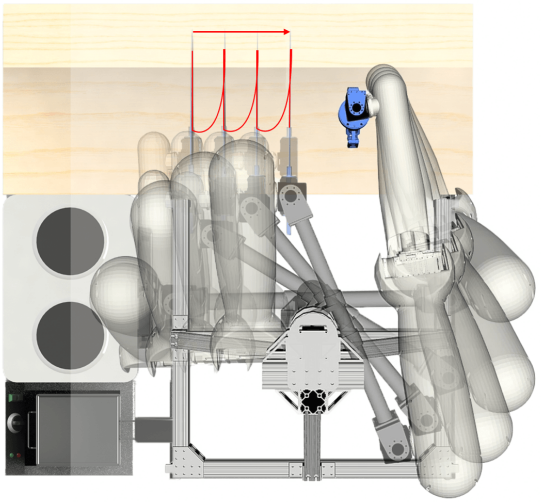

Fig. 11. Manipulator system making multiple parallel cuts with linear knife trajectories shown in red.

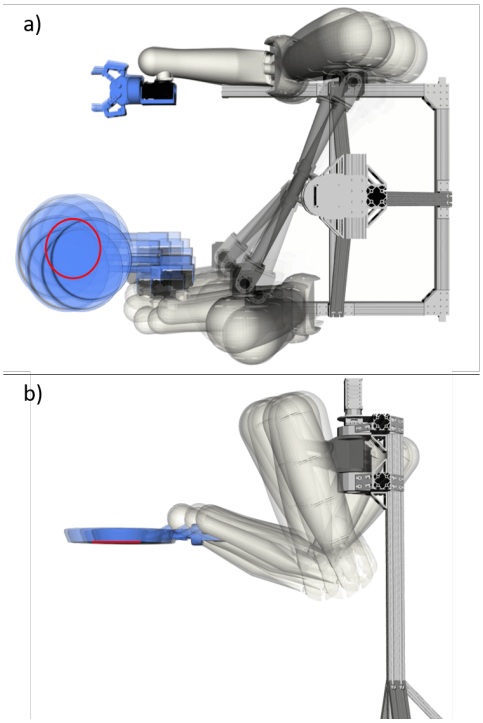

Fig. 12. Manipulator system making simple circles with the pan in a single plane with the pan trajectory shown in red. Viewed from the top (a) and from the side (b).

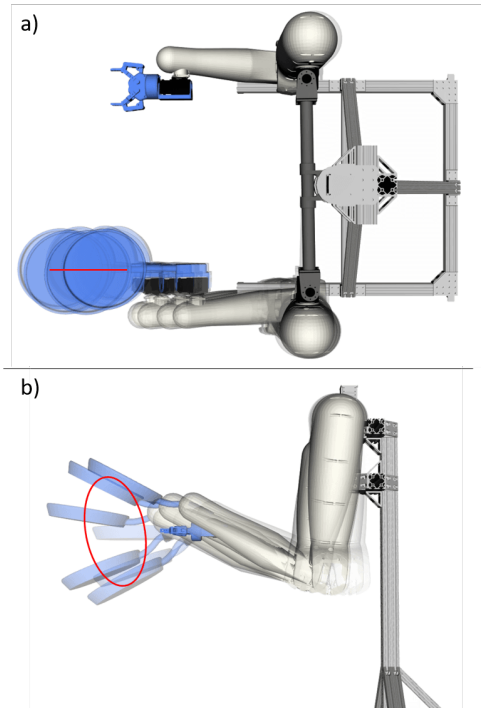

Fig. 13. Manipulator system making a complex 3D trajectory while simultaneously rotating the pan to simulate traditional human flipping motions seen in stir-frying with the pan trajectory shown in red. Viewed from the top (a) and from the side (b).

though, it is demonstrated through simulation that we can still produce parallel cuts with our 5 DOF arms coupled with the extra body DOF. A simulated cutting trajectory was laid out and simulated. The results of which are shown in Fig. 11. Here the redundant pitch DOF provided by the body joint allows the manipulator to produce the planar linear motions necessary for keeping the knife cuts parallel to each other. With only a 5 DOF arm on its own, the cuts would begin to angle radially about the shoulder joint of the robot. This would make uneven pieces and could lead to uneven doneness of the final cooked dish and would mitigate the potential advantages of the increased positional accuracy of robotic cooking.

Another common but often complex operation the manipulator was designed to replicate is the process of pan cooking. Commonly used in Chinese cuisine, moving the cooking pan in a precise nature to ensure even heating and mixing of ingredients have been carefully recreated by single tasking cooking devices [7], [21]. Fig. 12 and Fig 13, illustrate the next two trajectories simulated representing two key motions needed in stir-frying. In Fig 12, the manipulator demonstrates its ability to create accurate planar circular trajectories. In Fig. 13, the system recreates a pan flipping motion, commonly used in stir-frying. These kinds of movements will be necessary for the manipulator to accurately recreate cooking actions which are traditionally centered around the typical capabilities of human motion.

Lastly the robot's ability to multitask in a semi-structured environment was simulated. As humans we often take for granted our ability to easily move between workspaces when multitasking. However, this is not necessarily a straightforward task for traditional humanoid robots in unstructured or semi-structured environments [19], [20]. For example, when it became necessary to access another portion of the kitchen to procure a forgotten ingredient while cooking on the stove. For a human, the task is easily achieved with our strengths in vision and positioning. For a robot though, to precisely reposition itself in the kitchen and then return to the original position and regrasp its tool could be a time intensive process, which in cooking could lead to the dish being ruined. The inclusion of the body joint greatly expands the manipulator's workspace and allows it to move its arms independently to different quadrants of said workspace. This, along with careful consideration of link lengths, allows the manipulator to forgo repositioning itself when adding additional tasks and to be able to work on two potentially unrelated tasks in different work areas at one time. These features allow the manipulator to cook more quickly and efficiently. This was explored in simulation, shown in Fig. 14, by having the system cook with a frying pan over a stove using a circular trajectory to evenly cook its ingredients on one side of the cooking environment, while simultaneously reaching across with its other end-effector to grab a spice container. The robot brings the spice container from one side of the cooking area to the other to deliver the spices to the pan, without interrupting its second task of maintaining prior described circular pan trajectory.

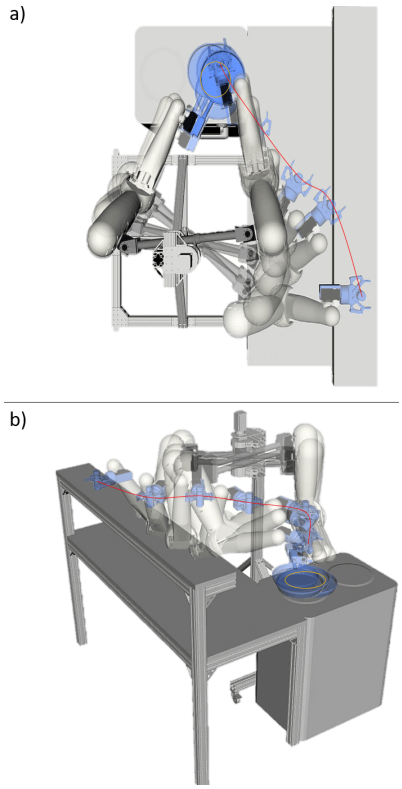

Fig. 14. Manipulator system demonstrating multitasking abilities by rotating a pan above a stove-top while retrieving and then depositing a spice container. The trajectory of the right arm is in red and the trajectory of the left arm is in orange. Viewed from a) the top and b) isometrically.

VI. CONCLUSION

This paper has laid out the factors considered in the design of a novel dual-arm manipulation platform optimized for preforming complex cooking tasks in a structured kitchen environment. This 11 DOF manipulator system is composed of two 5 DOF arms connected to an additional degree of freedom allowing the arms to rotate about the axis of the body of the robot. This allows the system to achieve a similar workspace to two 6 DOF arms, without the added weight, cost, and computational complexity of control. The central body degree of freedom allows for the expansion of the common workspace between the two arms allowing for the robot to perform dual armed tasks in any of the work areas surrounding the robot. Additionally, it gives the system a redundant pitch degree which allows for the arms to follow tricky trajectories such as planar circles and linear motions.

Moving forward, we will begin to test the physical system built off of this design. This will include a wide variety of tasks, from programming many of the essential cooking tasks addressed in Table 1 in the intro, to implementing force control for tasks involving deformable ingredients, to implementing vision feedback to augment the position feedback provided by the servo motors. Once the design is fully verified we will continue to iterate on the system. The primary upgrade being considered is the replacement of the current position controlled servo motors with proprioceptive actuators. Additionally, we will develop a new arm linkage system to allow more of the actuators to be located at the shoulder joint in order to further lower the mass inertia of each arm without sacrificing degrees of freedom. This will increase the maximum payload each arm is capable of lifting. This will all build towards creating a fully autonomous cooking system capable of producing a wide variety of high quality meals.

REFERENCES

[1] J. Wallén, *The history of the industrial robot*. Linköping University Electronic Press, 2008.
[2] M. E. Moran, "Evolution of robotic arms," *Journal of robotic surgery*, vol. 1, no. 2, pp. 103–111, 2007.
[3] M. Beetz, U. Klank, A. Maldonado, D. Pangercic, and T. Rühr, "Robotic roommates making pancakes-look into perception-manipulation loop," in *IEEE International Conference on Robotics and Automation (ICRA), Workshop on Mobile Manipulation: Integrating Perception and Manipulation*, 2011, pp. 9–13.
[4] W. Yan, Z. Fu, Y. Liu, Y. Zhao, X. Zhou, J. Tang, and X. Liu, "A novel automatic cooking robot for chinese dishes," *Robotica*, vol. 25, no. 4, pp. 445–450, 2007.
[5] D. Dong, "Robotic cooking system," Feb. 13 2007, uS Patent 7,174,830.
[6] T. J. Wang, "Automatic cooking device," Feb. 3 2009, uS Patent 7,485,830.
[7] Y. Chen, B. Li, and Z. Deng, "Dynamic modeling and performance analysis of a 3-dof pan mechanism for a cooking robot#," *Mechanics based design of structures and machines*, vol. 38, no. 2, pp. 243–260, 2010.
[8] (2020) Octochef. [Online]. Available: https://connected-robotics.com/en/product/octochef.html
[9] (2020) Moley robotics. [Online]. Available: https://www.moley.com/
[10] (2020) Samsung bot chef. [Online]. Available: https://news.samsung.com/global/get-a-glimpse-of-the-next-generation-innovations-on-display-at-samsungs-technology-showcase
[11] (2020) Lg cloi chefbot. [Online]. Available: https://www.lghvacstory.com/ces-2020-impresses-with-the-best-to-come-in-2020/
[12] (2020) Misorobotics flipy. [Online]. Available: https://misorobotics.com/
[13] X. Mu, Y. Xue, and Y.-B. Jia, "Robotic cutting: Mechanics and control of knife motion," in *2019 International Conference on Robotics and Automation (ICRA)*. IEEE, 2019, pp. 3066–3072.
[14] B. Li, Y. Chen, Z. Deng, and W. Xu, "Conceptual design and analysis of the 2t1r mechanism for a cooking robot," *Robotics and Autonomous Systems*, vol. 59, no. 2, pp. 74–83, 2011.
[15] M. Higashimori, K. Utsumi, Y. Omoto, and M. Kaneko, "Dynamic manipulation inspired by the handling of a pizza peel," *IEEE Transactions on Robotics*, vol. 25, no. 4, pp. 829–838, 2009.
[16] K. S. M. Schurr, G. Buess, "Robotics in endoscopic surgery: Can mechanical manipulators provide a more simple solution for the problem of limited degrees of freedom?" *Minimally Invasive Therapy & Allied Technologies*, vol. 10, no. 6, pp. 289–293, 2001.
[17] R. C. Dorf, *Systems, controls, embedded systems, energy, and machines*. CRC press, 2016.
[18] Q. Liu, C.-Y. Chen, C. Wang, and W. Wang, "Common workspace analysis for a dual-arm robot based on reachability," in *2017 IEEE International Conference on Cybernetics and Intelligent Systems (CIS) and IEEE Conference on Robotics, Automation and Mechatronics (RAM)*. IEEE, 2017, pp. 797–802.
[19] Y. Watanabe, K. Nagahama, K. Yamazaki, K. Okada, and M. Inaba, "Cooking behavior with handling general cooking tools based on a system integration for a life-sized humanoid robot," *Paladyn, Journal of Behavioral Robotics*, vol. 4, no. 2, pp. 63–72, 2013.
[20] W. Y. Z. F. Jiaxin Zhai, Gen Pan and Y. Zhao, "Dynamic analysis of a dual-arm humanoid cooking robot," in *2015 IEEE 10th Conference on Industrial Electronics and Applications (ICIEA)*. IEEE, 2015, pp. 835–838.
[21] H. Wang, W. Zhao, B. Li, X. Lin, and D. Zhang, "Dynamic analysis and robust reliability design of pan mechanism for a cooking robot," in *2009 IEEE International Conference on Robotics and Biomimetics (ROBIO)*. IEEE, 2009, pp. 1996–2001.